Development 133, 3907-3917 (2006) doi:10.1242/dev.02584

MES-4: an autosome-associated histone methyltransferase that participates in silencing the X chromosomes in the *C. elegans* germ line

Laurel B. Bender[1,*,†], Jinkyo Suh[1,*], Coleen R. Carroll[1,*], Youyi Fong[1,‡], Ian M. Fingerman[2], Scott D. Briggs[2], Ru Cao[3], Yi Zhang[3], Valerie Reinke[4] and Susan Strome[1,†]

Germ cell development in *C. elegans* requires that the X chromosomes be globally silenced during mitosis and early meiosis. We previously found that the nuclear proteins MES-2, MES-3, MES-4 and MES-6 regulate the different chromatin states of autosomes versus X chromosomes and are required for germline viability. Strikingly, the SET-domain protein MES-4 is concentrated on autosomes and excluded from the X chromosomes. Here, we show that MES-4 has histone H3 methyltransferase (HMT) activity in vitro, and is required for histone H3K36 dimethylation in mitotic and early meiotic germline nuclei and early embryos. MES-4 appears unlinked to transcription elongation, thus distinguishing it from other known H3K36 HMTs. Based on microarray analysis, loss of MES-4 leads to derepression of X-linked genes in the germ line. We discuss how an autosomally associated HMT may participate in silencing genes on the X chromosome, in coordination with the direct silencing effects of the other MES proteins.

KEY WORDS: *C. elegans*, MES proteins, Histone methylation, Germ line, X-chromosome silencing

INTRODUCTION

The modulation of chromatin structure has emerged as a key level of regulation of gene expression in many tissues and stages of development (e.g. Stillman and Stewart, 2004). One level of chromatin modulation is via the covalent modification of histones, including methylation, acetylation and ubiquitination (reviewed by Fischle et al., 2003). Modified histone residues can serve as docking sites for downstream effector proteins: for instance, H3 methylated at Lys9 recruits HP1, and H3 methylated at Lys27 recruits the Polycomb repressive complex PRC1 (reviewed by Martin and Zhang, 2005). Certain histone modifications are known to lead to either the activation or repression of underlying genes (Fischle et al., 2003; Sims et al., 2003).

Within the germ line of *Caenorhabditis elegans*, both X chromosomes in XX hermaphrodites and the single X in XO males are silenced by global repression mechanisms involving modifications of histones (Kelly et al., 2002). The *C. elegans* proteins MES-2, MES-3, MES-4 and MES-6 have been implicated in this repression. Mutations in the *mes* genes result in maternal-effect sterility, due to defects in germ cell proliferation and necrotic degeneration of germ cells (Capowski et al., 1991; Garvin et al., 1998). Several findings suggest that this necrotic germline death is primarily a result of the aberrant expression of X-linked genes when silencing fails. First, *mes* mutant animals with two X chromosomes are more severely affected than *mes* mutants with only one X; in fact, single X animals are usually fertile (Garvin et al., 1998). Second, in germ cells of wild-type hermaphrodites the X chromosomes lack numerous marks of active chromatin (Kelly et al., 2002), whereas in germ cells of *mes-2*, *mes-3* or *mes-6* hermaphrodites the X chromosomes display those marks (Fong et al., 2002). Thus, the MES proteins are required for germ cell viability and probably function, at least in part, to silence the X chromosomes.

MES-2, MES-3 and MES-6 operate together in a complex (Ketel et al., 2005; Xu et al., 2001) and probably participate directly in X-chromosome silencing. MES-2 possesses a SET domain, a hallmark of histone methyltransferases (HMTs), and has been shown to have HMT activity on Lys27 of histone H3 (H3K27) (Bender et al., 2004), like its fly and vertebrate orthologs, E(Z) and EZH2, respectively (Cao et al., 2002; Czermin et al., 2002; Kuzmichev et al., 2002; Muller et al., 2002). The HMT activity of MES-2 requires the association of both MES-6, an ortholog of fly ESC and vertebrate EED, and MES-3, a novel protein (Ketel et al., 2005). Thus, the MES-2/MES-3/MES-6 complex resembles the Polycomb Repressive Complex PRC2 in its HMT activity, substrate specificity and certain partner requirements. In worms, the MES-2/MES-3/MES-6 complex is responsible for all detectable H3K27 methylation in most regions of the germ line and in early embryos (Bender et al., 2004). Notably, the MES-2/MES-3/MES-6 complex concentrates trimethylated H3K27 (H3K27me3) on the X chromosomes (Bender et al., 2004). This repressive mark is likely to contribute to the repressed state of the X chromosomes (Fong et al., 2002).

The function of MES-4 has until now been a mystery. MES-4 shows the unique property of associating with the five autosomes but not with the X chromosome (Fong et al., 2002). Here, we show that MES-4 is a histone H3 HMT that it is responsible for all detectable H3K36 dimethylation in most regions of the germ line and in early embryos, and that it concentrates H3K36me2 marks on the autosomes. In contrast to Set2-related H3K36 HMTs, which associate with elongating RNA polymerase II and methylate H3K36 within the coding regions of genes (e.g. Kizer et al., 2005; Morris et al., 2005), the binding of MES-4 to chromatin and its H3K36 HMT

[1]Department of Biology, Indiana University, Bloomington, IN 47405, USA. [2]Department of Biochemistry, Purdue Cancer Center, Purdue University, West Lafayette, IN 47907, USA. [3]Department of Biochemistry and Biophysics, Lineberger Comprehensive Cancer Center, University of North Carolina at Chapel Hill, NC 27599, USA. [4]Department of Genetics, Yale University School of Medicine, New Haven, CT 06520, USA.

*These authors contributed equally to this work
[†]Authors for correspondence (e-mail: lbender@indiana.edu; sstrome@indiana.edu)
[‡]Present address: Department of Biostatistics, University of Washington, Seattle, WA 98195, USA

Accepted 8 August 2006

activity do not appear to depend on RNA polymerase II. This suggests that methylation of H3K36 can serve different roles in regulating chromatin function. Microarray analysis, performed on gonads dissected from wild type and *mes-4* mutants, revealed that loss of MES-4(+) function results primarily in the upregulation of genes on the X chromosome. Our results suggest that in germline tissue MES-4 cooperates with MES-2/MES-3/MES-6 to achieve proper silencing of X-linked genes.

MATERIALS AND METHODS

Worm strains

C. elegans N2 variety Bristol was used as the wild type. The following mutations, balancers, and translocations were used.
LGII: *rol-1(e91)*, *mes-2(bn11)*, *mnC1*.
LGIV: *mes-6(bn38)*, *DnT1(IV;V)*, *DnT1[qIs51](IV;V)*.
LGV: *dpy-11(e224)*, *mes-4(bn23, bn50, bn58, bn67, bn73, bn85, bn87)*, *pgl-3(bn104)*, *mnT12(IV;X)*.

RNAi analysis

RNAi was performed to deplete RNA Pol II/AMA-1, CDK-9 and TLK-1 as described by Kamath et al. (Kamath et al., 2003). Either wild-type or *mes-4(bn73)* L3 hermaphrodites were placed on plates containing dsRNA-expressing bacteria, at room temperature, and stained 36-40 hours later.

Immunofluorescence staining

Samples were fixed using methanol/paraformaldehyde (Han et al., 2003) or methanol/acetone (Strome and Wood, 1983). Rabbit antibodies to MES-4 were raised against the C-terminal 19 amino acids+Cys, or against amino acids 530-898, then affinity purified and used at 1:100 to 1:500 dilution. Other primary antibodies used were affinity-purified rabbit anti-H3K36me2 (Tsukada et al., 2006) at 1:200, mouse monoclonal antibody H5 to RNA Pol II CTD pSer2 (Covance) at 1:200, rabbit anti-H4K20me2 [Upstate and a gift from Yi Zhang (Fang et al., 2002)] at 1:100, chicken anti-H3K27me2 (Upstate) at 1:25, rabbit anti-H3K27me3 (Upstate) at 1:200, rabbit anti-acetylated histone H4 (Upstate) at 1:5000, mouse monoclonal antibodies PA3 at 1:1000 and PL4-2 at 1:2000 [a gift from M. Monestier (Monestier et al., 1994)], mouse monoclonal antibody OIC1D4 (Hird et al., 1996) at 1:5, and rat anti-PGL-3 (Kawasaki et al., 2004) at 1:10,000. Secondary antibodies from Jackson Immunologicals (TRITC-conjugated anti-rabbit IgG and anti-mouse IgM) and Molecular Probes (Alexa 488-conjugated anti-rat and anti-rabbit IgG) were used at 1:200. Images were acquired with an UltraVIEW LCI spinning-disk confocal laser and Nikon Eclipse TE200 microscope with UltraVIEW software (Perkin-Elmer), assembled with Adobe Photoshop, and displayed as projections of images taken at 0.5 μm intervals through the sample.

Bacterial expression of MES-4 and HMT assays

Full-length *MES-4* cDNA was subcloned into a pET28b bacterial expression vector (Novagen). Transformed BL21-Gold (DE3) *E. coli* were grown to an OD_{600} of 0.6 and induced with 0.1 mM isopropyl-D-thiogalactoside for 24 hours at 20°C. His-tagged MES-4 was detected in western blots using mouse monoclonal SC-8036 anti-His antibodies (Santa Cruz Biotechnology). HMT assays were performed by incubating 4 μl of bacterial lysate with 16 μg of chicken oligonucleosomes and 1.0 μCi of S-adenosyl-L-[methyl-^{3}H]methionine (Amersham Pharmacia Biotech) in methyltransferase buffer (25 mM Tris-HCl pH 8.0, 5% glycerol) for 30 minutes at 20°C in a total volume of 20 μl. Half of the reaction was analyzed by SDS-PAGE, followed by Coomassie staining and fluorography.

Microarray analysis of RNA from dissected gonads

Dissection of gonad arms from hermaphrodites, isolation of RNA, and linear amplification were performed as described by Chi and Reinke (Chi and Reinke, 2006). Gonad arms were dissected from wild-type and *mes-4*(*bn85*) M^+Z^- young adult hermaphrodites containing one to two fertilized embryos. During each of four dissection sessions, 100 gonad arms were collected from each genotype. Fluorescently labeled cDNA samples were prepared and hybridized to microarrays as previously described (Reinke et al., 2000). DNA microarrays were prepared as described elsewhere (Jiang et al., 2001; Reinke et al., 2004). Two hybridization experiments were performed with Cy3-labeled wild-type cDNA and Cy5-labeled *mes-4* cDNA, and two with the dyes swapped. For every gene in each microarray hybridization experiment, the ratio of wild type (wt)/*mes-4* was transformed into a $\log_2$ value and the mean $\log_2$ ratio calculated. Confidence levels were determined using a two-tailed paired *t*-test. Genes were considered to be significantly altered in the level of mRNA accumulation in wild type versus *mes-4* if they displayed a mean fold-difference ratio of 1.8 or higher, and a confidence level of greater than 95% ($P<0.05$) (Whetstine et al., 2005). The GEO accession number for microarray data is GSE5454.

Real-time PCR analysis of RNA from dissected gonads

Fifty gonad arms were dissected from wild-type and *mes-4(bn85)* M^+Z^- young adult hermaphrodites and total RNA isolated as described by Chi and Reinke (Chi and Reinke, 2006). Poly-adenylated cDNA was prepared using the SuperScript First-Strand Synthesis System for RT-PCR (Invitrogen). Real-time PCR was performed in triplicate using iQ SYBR Green Supermix (Bio-Rad) and the iCycler iQ Multi-Color Real-Time PCR Detection System (Bio-Rad). The Autoprime program (www.autoprime.de) was used to design primers to span an exon-exon junction. All data were normalized to *him-3* and F14B4.2, and the Pfaffl method (Pfaffl, 2001) was used to calculate relative fold changes.

RESULTS

MES-4 is a histone H3 lysine 36 methyltransferase

The presence in MES-4 of a SET domain (Fong et al., 2002) predicted that it has histone methyltransferase (HMT) activity. The mouse SET-domain protein bearing the closest similarity to MES-4 (Fong et al., 2002), NSD1, has been reported to methylate histones H3 and H4 in vitro (Rayasam et al., 2003). As shown in Fig. 1A, full-length 6his::MES-4 expressed in bacteria and incubated with chicken oligonucleosomes methylates H3. No other histones are detectably methylated.

We used antibodies specific for H3 and H4 peptides containing methylated lysines to investigate the residue specificity of MES-4. Mouse NSD1 has been reported to dimethylate H3K36 and H4K20 (Rayasam et al., 2003). Based on the staining of dissected *C. elegans* germ lines and early embryos with an antibody specific for H3 dimethylated at K36 (H3K36me2) (Tsukada et al., 2006), this mark is abundant on chromatin in wild-type worms but is absent from *mes-4* mutants (Fig. 1B-I). Thus, MES-4 is required for H3K36 dimethylation in vivo, at least in germline tissue (see below). Given its H3 HMT activity in vitro, we propose that MES-4 functions as an H3K36 HMT in vivo. Based on the staining of wild type and *mes-4* mutants, MES-4 is not required in vivo for any of the other H3 methyl marks we tested (H3K4me2 or me3, H3K9me2, H3K27me2 or me3, H3K79me2) or for H4K20me2 (Fong et al., 2002) (see Fig. S2E,F in the supplementary material; data not shown). The latter result agrees with the lack of H4 HMT activity of MES-4 in vitro. Furthermore, we were unable to detect H4 methylation activity for recombinant human NSD1 (amino acids 1556-1950) in vitro under conditions where strong H3 methylation was seen (data not shown). Therefore, we propose that both MES-4 and human NSD1 are specific for histone H3K36.

MES-4 is required for H3K36 dimethylation in most regions of the germ line and in early embryos

We used the antibody specific for H3K36me2 to investigate the tissue distribution of H3K36 dimethylation. H3K36me2 is abundant on the chromatin of most or all nuclei in wild-type worms (Fig. 1B-I; see also Fig. S1A in the supplementary material). To learn which tissues and stages require MES-4

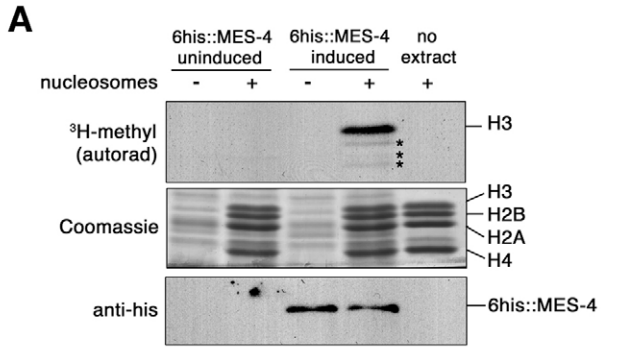

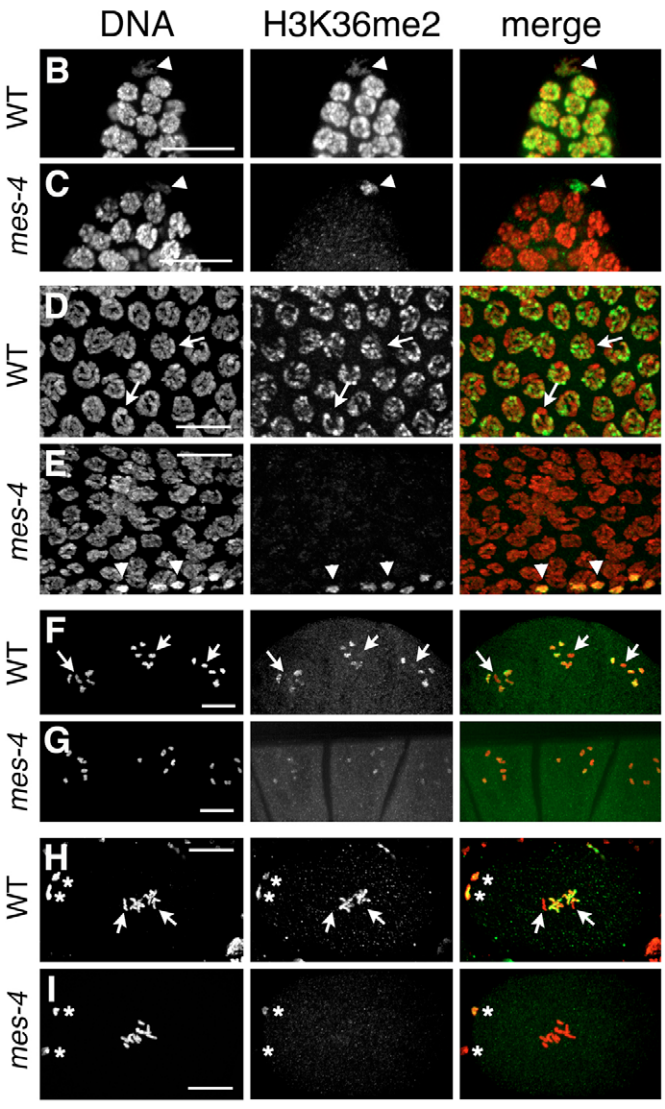

Fig. 1. MES-4 is a histone methyltransferase for H3K36. (**A**) MES-4 has HMT activity in vitro. Bacterially expressed His-tagged MES-4 was incubated with chicken oligonucleosomes and S-adenosyl-L-[methyl-^{3}H] methionine. The reaction products were analyzed by SDS-PAGE followed by fluorography (top panel) and Coomassie staining (middle panel). Western blots (bottom panel) were performed on the soluble extracts to detect MES-4. Asterisks mark H3 breakdown products in lane 4. (**B-I**) H3K36me2 is undetectable in *mes-4(bn73)* hermaphrodite germ lines and early embryos. Chromatin (labeled DNA) stained with PA3, red; H3K36me2 staining, green. Arrowheads mark somatic nuclei; arrows indicate X chromosomes. (B,C) Wild-type and *mes-4* distal gonads. (D,E) Wild-type and *mes-4* pachytene nuclei. (F,G) Wild-type and *mes-4* oocytes. (H,I) Wild-type and *mes-4* one-cell embryos. Anterior is to the left. Asterisks mark polar bodies. Scale bars: 10 μm.

function, we compared the H3K36me2 patterns in wild type to those in *mes-4* adult hermaphrodites, specifically in the fertile F1 progeny of *mes-4*/+ heterozygotes. These F1 progeny have a maternal load of *mes-4* products but no expression from the zygotic genome (we refer to them as M^+Z^-). The embryos produced by M^+Z^- hermaphrodites are M^-Z^- and develop into sterile adults. In *mes-4* M^+Z^- germ lines, H3K36me2 is undetectable in nuclei from the mitotically dividing distal region of the gonad (Fig. 1C) through the pachytene region (Fig. 1E). Some H3K36me2 signal is visible in late-pachytene/diplotene nuclei and in oocytes (Fig. 1G). In addition, some H3K36me2 staining is detectable in the polar body products of oocyte meiosis, although H3K36me2 staining is undetectable in the blastomere nuclei of *mes-4* embryos through the ~35-cell stage (Fig. 1I, see Fig. 4B). Thus, MES-4 is responsible for all detectable H3K36 dimethylation in most regions of the adult germ line and in early stages of embryogenesis. A different H3K36 HMT(s) apparently is active in adult somatic cells (arrowheads in Fig. 1C,E), in the diplotene/diakinesis region of the oogenic germ line, and in >40-cell-stage embryos (Fig. 4D,F,H). These findings are consistent with the accumulation of MES-4 in the germ line and in early embryos (Fong et al., 2002), and with *mes-4* mutants displaying defects primarily in the germ line (Capowski et al., 1991).

MES-4 and H3K36me2 are restricted to the autosomes and the left tip of the X chromosome

A striking feature of the wild-type H3K36me2 pattern in germline and early embryo nuclei is that a pair of chromosomes lacks this mark (Fig. 1D,H) and one oocyte bivalent has low levels of this mark (Fig. 1F). Because MES-4 is dramatically enriched on autosomes (Fong et al., 2002), we predicted that the chromosomes lacking H3K36me2 are the X chromosomes. H3K36me2 staining of X:autosome translocations in embryos confirmed that prediction: H3K36me2 is absent from the presumed X-chromosome portion of each translocation chromosome (Fig. 2B). Interestingly, in embryos containing an X:autosome translocation with a free left end of the X chromosome, we noticed a pinpoint spot of MES-4 (or of H3K36me2) staining on the exposed tip of the X portion (Fig. 2A,B). A 'dot' of MES-4 was detected on 16 out of 31 X-chromosome left ends examined. A dot of MES-4 was never found on the right end (18 X-chromosome right ends examined; data not shown). Clues as to the significance of the dot of X-chromosome staining are considered in the Discussion.

Targeting of MES-4 to chromosomes requires the first PHD finger

MES-4 contains three CysHis fingers previously classified as PHD (plant homeodomain) motifs, plus an AWS-like domain and a post-SET domain flanking the SET domain (Fong et al., 2002) (Fig. 3A). We sequenced seven EMS- or gamma radiation-induced *mes-4* mutations (Capowski et al., 1991; Fong et al., 2002) (Fig. 3A; see

also Table S1 in the supplementary material). Some of the *mes-4* lesions shed light on features of MES-4 required for its association with chromatin, in particular the first PHD domain.

Two point mutations in the first PHD finger, *bn50* and *bn67*, lead to an apparently complete dissociation of MES-4 from chromosomes (Fig. 3B, row 4; data not shown). PHD domains are predicted zinc-binding fingers and are considered to be a signature of chromatin-associated proteins (Bienz, 2006). Studies of ISWI and p300 implicate their PHD domains in nucleosome binding (Eberharter et al., 2004; Ragvin et al., 2004), and more recently the PHD domains of ING2 and of BPTF have been shown to bind H3K4me3 (Li et al., 2006; Pena et al., 2006). Although the first PHD domain of MES-4 is fairly atypical (Bienz, 2006), it appears to be crucial for MES-4 to associate with chromatin.

The in-frame deletion allele *bn85*, which disrupts the SET domain, results in partial dissociation of MES-4 from chromosomes (Fig. 3B, row 3; see Table S1 in the supplementary material). The small amount of *bn85* mutant protein bound to chromosomes does not lead to detectable H3K36me2 signal (data not shown). The partial dissociation of *bn85* protein from chromosomes may implicate the SET and/or post-SET domains in having a minor role in the localization of MES-4 to chromatin.

The point mutation *bn58*, within the region between the third PHD domain and the AWS-like domain, also results in partial dissociation of MES-4 from chromosomes (Fig. 3B, row 2). *bn58* is the only *mes-4* allele that displays detectable H3K36me2 signal (Table S1 in the supplementary material), suggesting that the fraction of mutant protein that is associated with chromatin has at least partial HMT activity. This residual activity may confer upon *bn58* animals the ability to produce more germ nuclei than other *mes-4* mutants (Capowski et al., 1991).

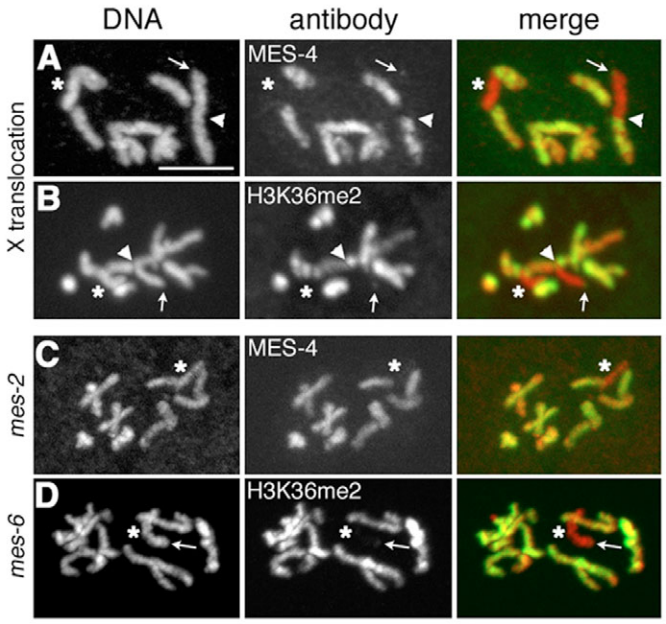

Fig. 2. MES-4 and H3K36me2 are concentrated on the autosomes in wild type and spread to the oocyte-derived X chromosome in *mes-2* and *mes-6* mutant embryos. One-cell embryos with oocyte-derived (anterior, left) and sperm-derived (posterior, right) pronuclei at pronuclear fusion. DNA is stained red with PA3 (A,B,D) or PL4-2 (C); MES-4 or anti-H3K36me2 staining is green. (**A**,**B**) Embryos bearing the translocation *mnT12 (IV;X)* in which the right end of the X chromosome is fused to the left end of chromosome IV. Arrowheads indicate IV;X junctions. Asterisks mark the X portion of the other fused chromosome. (**C**,**D**) *mes-2(bn11)* and *mes-6(bn38)* embryos. MES-4 and H3K36me2 are on the oocyte-derived X chromosome but are absent from the sperm-derived X (asterisk). Arrows in A,B,D indicate a dot of MES-4 or H3K36me2 at the tip of an X chromosome. Scale bar: 5 μm.

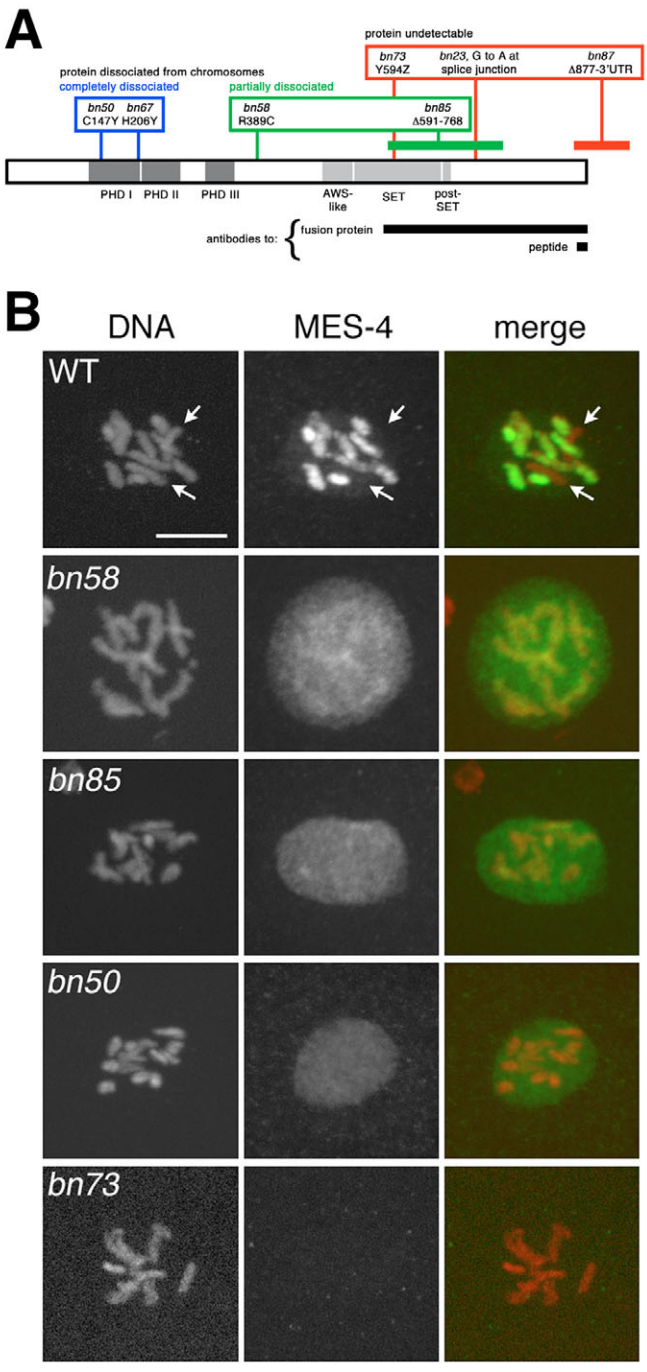

Fig. 3. *mes-4* mutant alleles and the resulting MES-4 distributions. (**A**) Locations and classifications of the lesions in seven *mes-4* alleles. Also see Table S1 in the supplementary material. (**B**) MES-4 distribution in one nucleus of two-cell wild-type and *mes-4* embryos. DNA is stained red with PL4-2 (row 5) or PA3 (all other rows); MES-4 is green. The arrows in the wild-type panels indicate unstained X chromosomes. Scale bar: 5 μm.

Exclusion of MES-4 and H3K36me2 from the X requires MES-2, MES-3 and MES-6, and also depends on gamete history

Previously we showed that the SET-domain protein MES-2, in a complex with MES-3 and MES-6, is required for H3K27 di- and trimethylation in the *C. elegans* germ line (Bender et al., 2004), and that MES-4 patterns are altered in *mes-2*, *mes-3* and *mes-6* mutants. Specifically, in *mes-2*, *mes-3* and *mes-6* M^+Z^- germ lines, MES-4 appears ectopically on X chromosomes in late oogenesis (Fong et al., 2002). Here, we have examined both MES-4 and H3K36me2 patterns in *mes-2*, *mes-3* and *mes-6* M^-Z^- early embryos (Fig. 2C,D). Consistent with our previous study, in early embryos MES-4, and also H3K36me2, spread to the oocyte-derived X chromosome. Thus, the activity of the MES-2/MES-3/MES-6 complex participates in repelling MES-4 and H3K36me2 from the X chromosomes at late stages of oocyte differentiation and in early embryos.

Curiously, in *mes-2*, *mes-3* and *mes-6* embryos, in contrast to the oocyte-derived X, the sperm-contributed X remains unstained (or is occasionally very faintly stained) by MES-4 and H3K36me2. After sperm chromatin is apparently stripped of histone modifications during spermatogenesis, an unidentified 'imprint' on the sperm X chromosome causes it to reacquire H3K4me and H3K9/K14ac (acetyl) marks several cell cycles later than the autosomes, which acquire those modifications shortly after fertilization (Bean et al., 2004). This imprint is likely to explain the failure of MES-4 and H3K36me2 to decorate the sperm X in *mes-2*, *mes-3* and *mes-6* mutants.

The MES-2/MES-3/MES-6 complex may repel MES-4 and its HMT activity not only from the oocyte-derived X chromosome but also from particular regions of the autosomes. The pattern of H3K36me2 on autosomes is patchy or banded in appearance in wild type (Fig. 1D, see also Fig. S2 in the supplementary material), and appears more uniform and intense in *mes-2*, *mes-3* and *mes-6* nuclei (Fig. 2, compare rows B and D; Fig. S2, compare rows A and B, and rows C and D). An attractive mechanistic model to explain this finding is that MES-2-catalyzed methylation of H3K27 prevents MES-4 from binding to and methylating a nearby residue of the H3 tail, K36.

Another H3K36 HMT becomes active by the ~40-cell stage of embryogenesis

Prior to the ~35-cell stage of embryogenesis in *mes-4* M^-Z^- embryos, no H3K36me2 is visible on chromosomes (Fig. 4B). As *mes-4* embryos reach the ~40-cell stage, several nuclei show a faint H3K36me2 signal (Fig. 4D). The intensity of staining increases as the embryos develop (Fig. 4F). These results demonstrate that at least one other H3K36 HMT, in addition to MES-4, becomes active in embryos. Notably, this non-MES-4 H3K36 HMT does not appear to be active in the primordial germ cell P4 or its newly formed daughters Z2 and Z3 (Fig. 4D,F), where MES-4 is active (Fig. 4C,E). Later, during the comma stage of embryogenesis, H3K36me2 appears in Z2 and Z3 of *mes-4* embryos (Fig. 4H). H3K36me2 levels are somewhat higher in all nuclei of older wild-type embryos and L1 larvae when compared with *mes-4* mutants (Fig. 4G,H), probably because of the contribution of MES-4 activity to overall levels of H3K36me2.

MES-4 HMT activity does not appear to be linked to transcription elongation

Because MES-4 is concentrated on autosomes, and because autosomes, but not X chromosomes, are actively transcribed in the germ line, we investigated whether MES-4 H3K36 HMT activity is

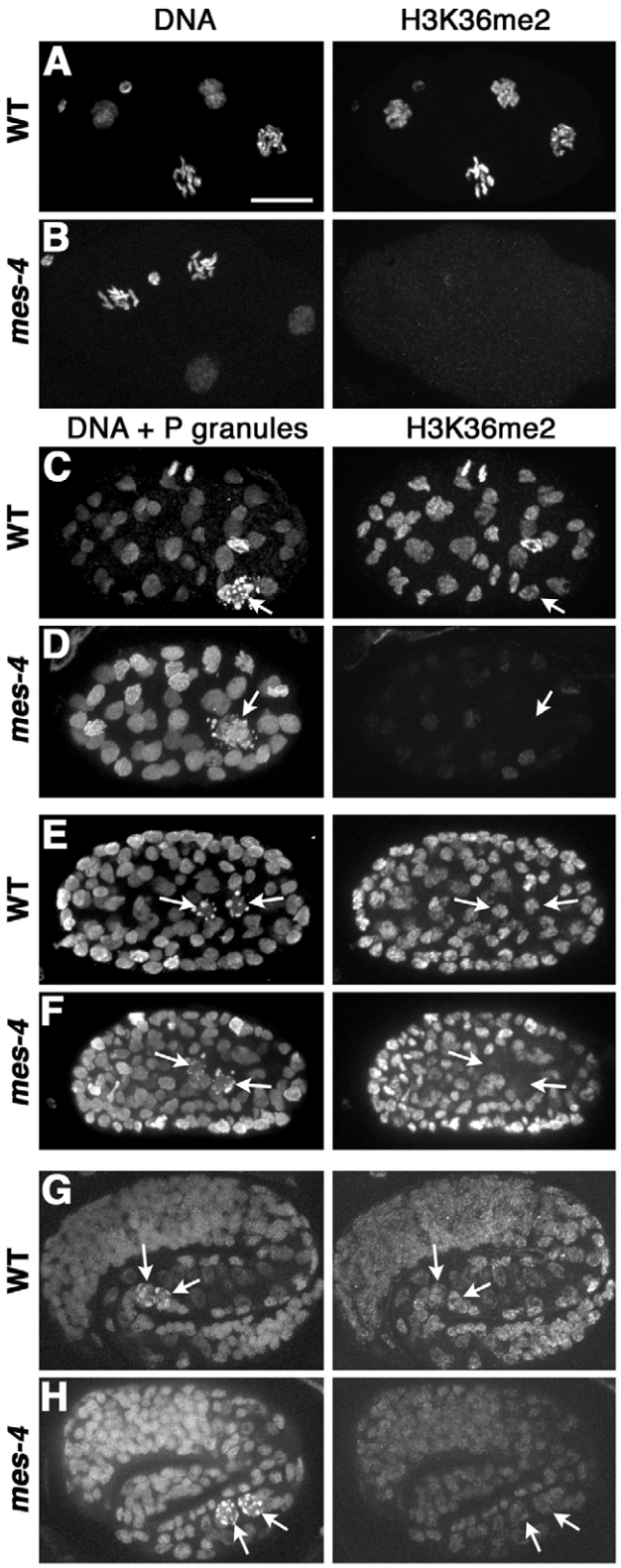

Fig. 4. MES-4 is responsible for all H3K36me2 in early embryos, but another HMT becomes active by the ~40-cell stage. DNA is stained with PL4-2 (G,H) or PA3 (all other rows). P granules are stained with monoclonal antibody OIC1D4 (Hird et al., 1996). Arrows indicate P-granule-containing primordial germ cells. Anterior is to the left. (**A**,**B**) Wild-type and *mes-4(bn73)* four-cell embryos. (**C**,**D**) ~40-cell embryos. (**E**,**F**) ~100-cell embryos. (**G**,**H**) Three-fold embryos. Scale bar: 10 μm.

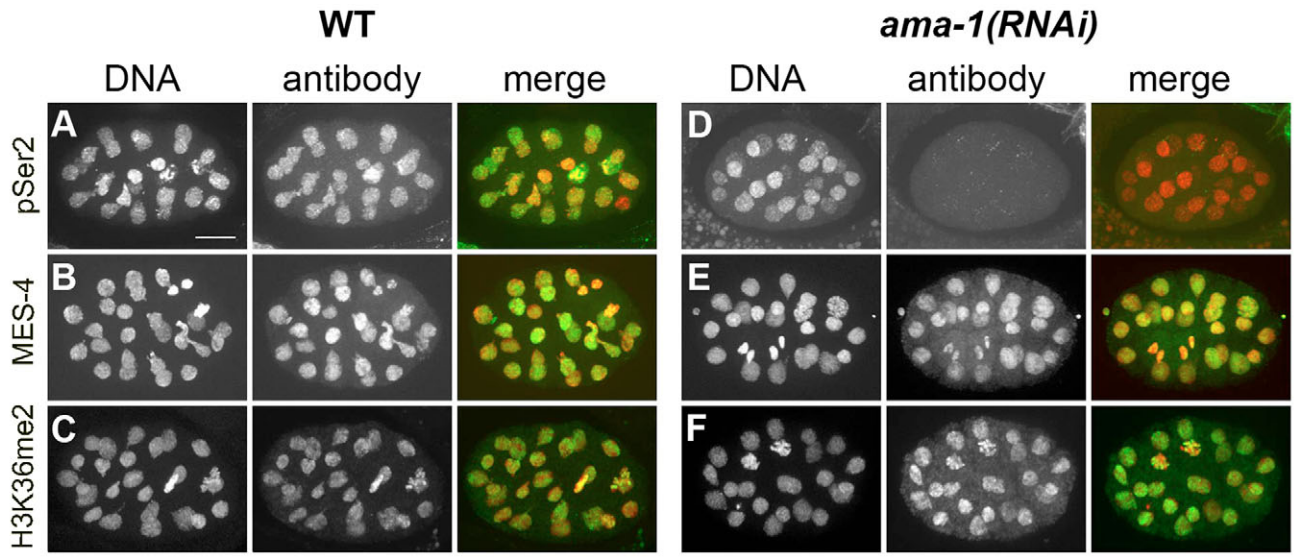

Fig. 5. MES-4 binding and methylation of H3K36 do not appear to depend on transcription elongation. Comparison of MES-4 and H3K36me2 distribution and levels in ~24-cell wild-type and *ama-1(RNAi)* embryos. Anterior is to the left. DNA is stained red with anti-acetylated H4 (A,D) or PA3 (B,C,E,F); staining of CTD Ser2 phosphorylation (pSer2), MES-4 and H3K36me2 is green. (**A-C**) Wild-type embryos. (**D**) *ama-1(RNAi)* embryo showing effective depletion of pSer2. (**E**,**F**) *ama-1(RNAi)* embryos showing apparently normal levels and distributions of MES-4 and H3K36me2. Scale bar: 10 μm.

directly associated with the progression of transcription. Studies in *Saccharomyces cerevisiae* showed that Set2, an H3K36 HMT, associates with the elongating form of RNA Pol II (Krogan et al., 2003; Li et al., 2002; Li et al., 2003; Schaft et al., 2003; Xiao et al., 2003). The emerging view is that Pol II phosphorylated on Ser2 of its C-terminal domain (CTD) recruits Set2, which in turns methylates nearby nucleosomes. Transcription elongation-coupled methylation of H3K36 appears to be widely conserved across eukaryotic species (Adhvaryu et al., 2005; Kizer et al., 2005; Morris et al., 2005; Sun et al., 2005).

To test whether MES-4-mediated H3K36 methylation is linked to transcription, we examined MES-4 localization and H3K36 methylation after RNAi depletion of the large subunit of Pol II, AMA-1, which contains the CTD. We focused on young embryos (<40 cells) in which all detectable H3K36 methylation requires MES-4 (see above). *ama-1(RNAi)* embryos lacked detectable CTD Ser2 phosphorylation (and in fact lacked detectable Pol II; not shown), but displayed normal-appearing MES-4 localization to chromosomes, and to autosomes in particular, and normal levels of H3K36me2 (Fig. 5A-F). Conversely, *mes-4* mutant embryos displayed apparently normal levels of CTD Ser2 phosphorylation (data not shown). These findings suggest that MES-4 association with chromatin and HMT activity are not directly linked to transcription elongation, and that MES-4-mediated H3K36 methyl marks serve a different role in *C. elegans* than Set2-mediated H3K36me marks.

To investigate whether the non-MES-4 H3K36 HMT activity that becomes active in >40-cell *C. elegans* embryos is linked to transcription elongation, we examined whether the residual H3K36me2 mark in >40-cell *mes-4* embryos is affected by *ama-1(RNAi)*. H3K36me2 was undetectable in *mes-4; ama-1(RNAi)* ~100-cell embryos (Fig. 6A-D). Depletion of CTD Ser2 kinases (CDK-9 or TLK-1) (Han et al., 2003; Shim et al., 2002) in a *mes-4* background also eliminated H3K36me2 signal (see Fig. S3 in the supplementary material), revealing that the residual H3K36me2 signal in *mes-4* embryos requires the phosphorylated form of CTD Ser2 in embryos. These results suggest that: (1) non-MES-4-mediated dimethylation of H3K36 is directly linked with transcription; and/or (2) the non-MES-4 H3K36 HMT must be transcribed from the embryonic genome.

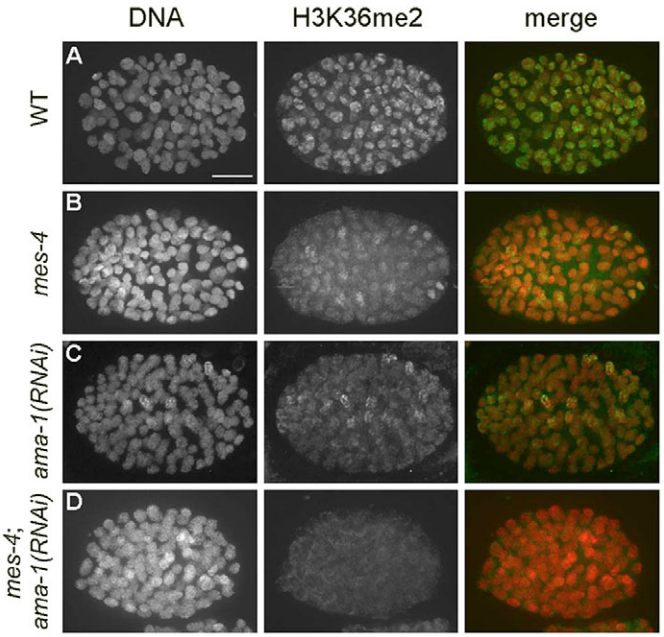

Fig. 6. Activity of the non-MES-4 H3K36 HMT(s) depends on transcription. Analysis of H3K36me2 levels in ~100-cell embryos lacking MES-4, AMA-1, or both. DNA is stained red with PA3; H3K36me2, green. (**A**) Wild-type embryo. (**B**,**C**) *mes-4(bn73)* and *ama-1(RNAi)* embryos display reduced H3K36me2 relative to wild type. (**D**) The *mes-4(bn73)*; *ama-1(RNAi)* embryo lacks detectable H3K36me2 signal. Scale bar: 10 μm.

Loss of MES-4 results in desilencing of X-linked genes

To investigate directly the impact of MES-4 chromatin regulation on gene expression, microarray analysis was used to compare the profile of mRNA accumulation in wild-type and *mes-4* mutant germ lines. Ideally, we would compare the nascent germ lines in young wild-type and M^-Z^- mutant larvae, prior to the onset of germline degeneration in mutants. Because those germ lines contain very few cells, we instead analyzed isolated gonads dissected from wild-type hermaphrodites and from fertile *mes-4* M^+Z^-hermaphrodites. Several observations justified analyzing the M^+Z^- generation. First, MES-4 levels are below detection in M^+Z^- adults (see Fig. S1C in the supplementary material). Second, as described above, MES-4-mediated H3K36me2 is also undetectable in M^+Z^- germ lines. Third, *mes-4* M^+Z^- germ lines are compromised: transgenes are desilenced, brood size is reduced, and RNAi depletion of other chromatin regulators renders *mes-4* M^+Z^- worms, but not wild-type worms, sterile (Capowski et al., 1991; Kelly and Fire, 1998; Xu and Strome, 2001). We reasoned that altered patterns of gene expression are likely to underlie these M^+Z^- germline phenotypes, and that elucidating the alterations would provide insights into MES-4 function.

Gonads from wild-type and *mes-4* M^+Z^- gravid hermaphrodites were dissected, RNA linearly amplified, and cDNA prepared and labeled with Cy3 and Cy5. Hybridizations were performed in quadruplicate to DNA microarrays representing ~16,400 of the ~20,000 predicted *C. elegans* genes (Reinke et al., 2004). Seventy-one genes displayed significantly different accumulation in *mes-4* relative to wild type (>1.8 average fold difference, $P<0.05$, two-tailed paired *t*-test, see Materials and methods; Fig. 7A,C; see also Table S2 in the supplementary material). The microarray results were validated by real-time PCR for 15 out of 15 genes ($P<0.05$) selected at random from the upregulated, downregulated, and non-regulated classes (see Table S3 in the supplementary material).

Two aspects of the altered gene expression profile in *mes-4* are particularly striking and informative. First, 67 of the 71 affected genes displayed higher expression (upregulated) in *mes-4* mutants relative to wild type, and four genes displayed lower expression

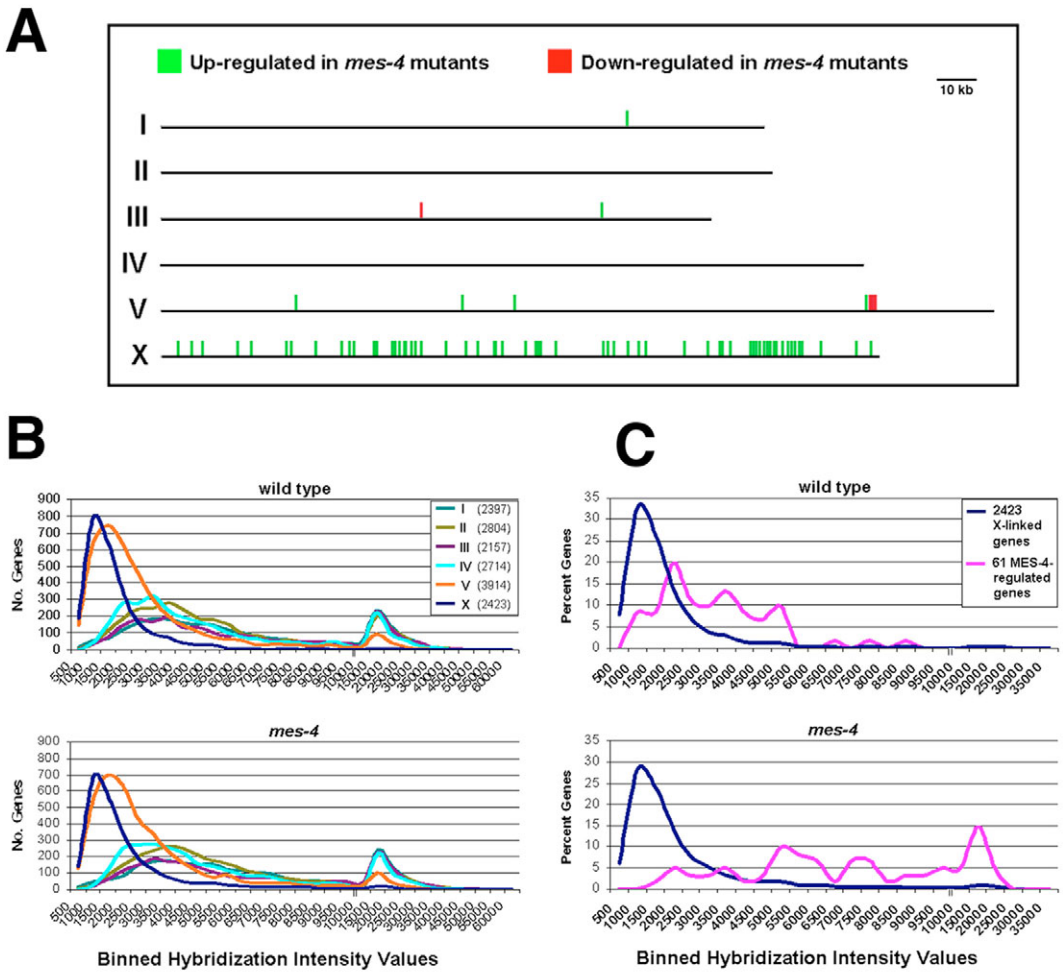

Fig. 7. Microarray analysis reveals derepression of X-linked genes in *mes-4* mutant germ lines. Microarray analysis was performed using linearly amplified RNA from gonads dissected from wild-type and *mes-4(bn85)* M^+Z^- adult hermaphrodites. (**A**) Green and red tick marks show the chromosomal positions of the 71 genes that are up- or downregulated at least 1.8-fold in *mes-4* mutants relative to wild type ($P<0.05$, two-tailed paired *t*-test). Green, 67 genes that are upregulated in *mes-4* mutant gonads; red, four genes that are downregulated in *mes-4* mutant gonads. Gene IDs and fold differences are shown in Table S2 in the supplementary material. (**B**) Histograms showing the number of genes on each chromosome that displayed various mean hybridization intensities. The total number of genes sampled on each chromosome is in parentheses in the key. (**C**) Histograms showing the percentage of X-linked genes that displayed various mean hybridization intensities. Pink, 61 X-linked genes that are upregulated >1.8-fold in *mes-4* mutant gonads; blue, all 2423 analyzed genes on the X chromosome. The units on the *x*-axis change at 10,000.

(downregulated). Second, 61 of the 67 genes upregulated in *mes-4* mutants are located on the X chromosome. Given the relative sizes of the six chromosomes and gene representation on our microarrays, random chance alone would predict that 10 of the 67 upregulated genes would map to the X. Thus, the primary effect of loss of MES-4 function on gene accumulation patterns in M^+Z^- germ lines is upregulation of genes on the X chromosome.

Given the concentration of MES-4 on autosomes, we considered the possibility that an apparent upregulation of genes on the X chromosome in fact reflects widespread downregulation of autosomal genes in *mes-4* mutants. In this scenario, MES-4 would serve as an activator of autosomal genes; loss of MES-4 would cause a reduced accumulation of autosomal transcripts and therefore of total mRNA, and our use of equivalent input mRNA to prepare microarray probes would result in artificially elevated levels of X-linked mRNAs. This scenario is highly unlikely for several reasons. (1) Absolute hybridization intensities for all ~16,400 genes represented on the microarrays showed similar profiles in wild type and *mes-4* mutants (Fig. 7B). (2) Given the banded appearance of MES-4 and H3K36me2 on the autosomes, downregulation of autosomal genes in *mes-4* mutants would be expected to show gene-to-gene variation. Only 10 autosomal genes of the ~14,000 represented on the microarrays showed a >1.8-fold difference in accumulation in *mes-4* gonads relative to in wild-type gonads, and only four of those were downregulated in *mes-4* mutants (Fig. 7A; see also Table S2 in the supplementary material). (3) If the downregulation of autosomal genes led to an apparent upregulation of X-linked genes in *mes-4* gonads, then those genes on the X chromosome would be expected to be fairly uniformly affected. Instead, only 61 of the ~2400 X-linked genes represented on the microarrays showed a >1.8-fold difference in accumulation in *mes-4* gonads relative to wild type. (4) Real-time PCR analysis using non-amplified RNA from 50 dissected *mes-4* and wild-type gonads verified the up- or downregulation of 10 genes, and the approximately equivalent accumulation of 5 genes (see Table S3 in the supplementary material).

Taken together, our results lead to the surprising conclusion that MES-4, a chromatin regulator concentrated on the five autosomes, functions to repress genes on the X chromosome. How X-chromosome silencing may be achieved by MES-4, in collaboration with the MES-2/MES-3/MES-6 complex, is discussed below.

DISCUSSION

MES-4 is an H3K36 methyltransferase in the germ line and in early embryos

Our in vitro HMT assays and in vivo staining results demonstrate that MES-4 methylates histone H3 on K36. The MES-4-related HMT, mouse NSD1, was reported to methylate H3K36 and, additionally, H4K20 (Rayasam et al., 2003). We do not see evidence that MES-4 participates in H4K20 methylation. Mouse NSD1 was further reported to methylate oligonucleosomes, core histones, and recombinant H3 and H4. In our assays, MES-4 and human NSD1 methylated oligonucleosomes, but not core histones or recombinant H3 or H4 (not shown). Our results suggest that both MES-4 and human NSD1 prefer nucleosomal substrates and are specific for H3K36. Mouse NSD1 may have a broader substrate range.

MES-4 is apparently the sole active H3K36me2 HMT in the regions of the germ line extending from the distal mitotic stem cells through the meiotic pachytene region. In those regions, MES-4 and H3K36me2 are excluded from all of the X chromosome except the leftmost tip (Fong et al., 2002) (this report), and the X chromosomes are silenced (Kelly et al., 2002). During oogenesis, the X chromosomes become at least partially activated late in pachytene (Kelly et al., 2002). This turn-on of the X chromosomes is not accompanied by a detectable appearance of MES-4 on them, which argues, as do our microarray results, against a model in which MES-4 is required to activate gene expression in the germ line. However, concomitant with X activation, an H3K36me2 HMT distinct from MES-4 becomes active on the X chromosomes as well as the autosomes, leading to methylation of H3K36 on all chromosomes. This non-MES-4 HMT may serve a Set2-like role during transcription elongation (e.g. Kizer et al., 2005).

In embryos, MES-4 remains autosomally concentrated until at least the 100-cell stage (data not shown), and is responsible for all detectable H3K36me2 until about the 40-cell stage, at which time another H3K36 HMT(s) also becomes active. The current view is that *C. elegans* early embryos inherit a large stockpile of maternal transcripts, initiate embryonic transcription of at least some genes by the four-cell stage, and undergo a 'mid-blastula transition' from maternal to embryonic control of development at about the 40-cell stage (Baugh et al., 2003; Edgar et al., 1994; Seydoux and Fire, 1994). Methylation of H3K36 catalyzed by the non-MES-4 HMT, which becomes detectable by the 40-cell stage, is temporally correlated with activation of the embryonic genome and may serve an essential role in that process. This non-MES-4 HMT(s) is dependent on Pol II and thus may function similarly to yeast Set2.

H3K36me2 marks may serve diverse roles

In the yeast *S. cerevisiae*, Set2 catalyzes all H3K36 methylation and requires association with Pol II for this activity (Strahl et al., 2002; Kizer et al., 2005). H3K36me2 in *S. cerevisiae* is recognized by the Rpd3S complex, which deacetylates nucleosomes within gene coding regions, to aid in suppressing aberrant intragenic transcription initiation (Carrozza et al., 2005; Joshi and Struhl, 2005; Keogh et al., 2005). H3K36me2 marks also may serve to distinguish actively transcribed sequences from inactive genes and from regulatory sequences in yeast and higher eukaryotes (Bannister et al., 2005; Rao et al., 2005; Sun et al., 2005).

Our studies suggest that MES-4 associates with and methylates chromatin independently of Pol II. This in turn suggests that MES-4-catalyzed methylation of H3K36 serves a role distinct from those described above. The same may be true of the MES-4-related proteins in humans: NSD1, NSD2/MMSET and NSD3. Significantly, all three have been implicated in causing or promoting human cancers when mutated or overexpressed (Schneider et al., 2002). Our findings on *C. elegans* MES-4 invite speculation that the NSD family HMTs may also operate independently of Pol II.

MES-4 and H3K36me2 on the left tip of the X chromosome

MES-4 and H3K36me2 both decorate autosomes in a banded pattern and are excluded from all regions of the X chromosome except the left tip. The left end of the X chromosome has emerged as being different from the remainder of the X in several respects. The meiotic pairing center for the X chromosome is located less than 2 Mb from the left end (MacQueen et al., 2005). This region binds to the zinc-finger protein HIM-8 and associates with the nuclear envelope during meiotic prophase (Phillips et al., 2005). The left end of the X is also enriched relative to the rest of the X chromosome for AA/TT dinucleotides that are periodically spaced along one face of the DNA helix, and that may influence DNA bending and chromatin structure (Fire et al., 2006). The X-chromosome left end also contains three copies of a 14 base pair perfect repeat that is distributed abundantly over the autosomes (696 copies total), but

found nowhere else on the X chromosome (I. Korf and J. Bedell, personal communication). Tests to date have not revealed an involvement of this 14-mer in MES-4 binding specificity (P. Poole, C.R.C. and S.S., unpublished).

In the germ line, MES-4 participates in silencing X-linked genes

Earlier observations that MES-4 is concentrated on the autosomes, and that in the germ line many autosomal genes are expressed, while the X chromosome is globally silenced, led to the expectation that MES-4 serves an activating role on autosomes. Our microarray results do not support that view and instead lead to the surprising conclusion that autosomally concentrated MES-4 somehow participates in repressing genes on the X chromosome. Although relatively few X-linked genes (61 of 2423 genes tested) were upregulated >1.8-fold in a *mes-4* background, this small number is likely to be a consequence of performing the analysis in the M^+Z^- generation. Such M^+Z^- *mes*-4 mutant hermaphrodites are fertile, and so, although germline health is compromised in these individuals (see Results), they were not expected to display dramatic alterations in mRNA profiles. We envision that the maternal load of wild-type *mes-4* gene product in young M^+Z^- worms and its epigenetic influences are sufficient to enable the nascent germ line to launch the normal pattern of gene expression, but that as the maternal load declines and development proceeds, transcription patterns become altered. We predict that the M^-Z^- offspring of M^+Z^- *mes-4* mothers will show earlier and more dramatic alterations in germline gene expression patterns. Given the small size of the nascent germ line (i.e. two cells in a newly hatched 550-cell larva), testing that prediction is challenging, but is a high priority.

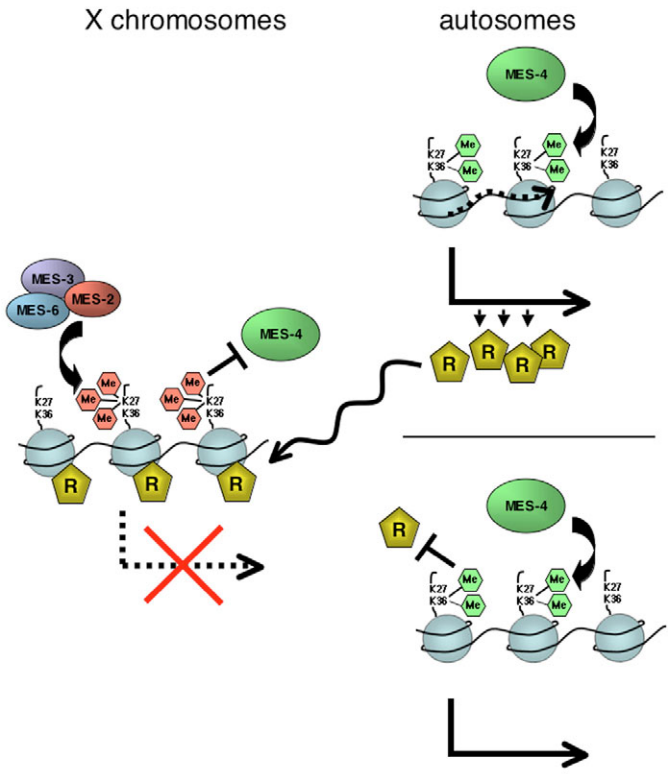

Fig. 8. Summary of MES-mediated histone methylation and models for the roles of the MES proteins in silencing the X chromosome in the germ line. (Left) The MES-2/MES-3/MES-6 complex catalyzes di- and trimethylation of H3K27, and preferentially concentrates H3K27me3 on the X chromosome (Bender et al., 2004). We hypothesize that MES-2/MES-3/MES-6 function repels MES-4 from the X chromosome and from regions of the autosomes (Fong et al., 2002) (this study). (Right) Two models for the role of MES-4. (Top right) MES-4 dimethylation of H3K36 in or near an autosomal gene (dotted line) activates that gene to express a repressor (labeled 'R') of many X-linked genes. (Lower right) MES-4 concentrates H3K36me2 on the autosomes; MES-4 or H3K36me2, in turn, repels a repressor (labeled 'R') from the autosomes, focusing its binding or action on the X chromosome. We speculate that the silencing of genes on the X chromosome is achieved by the combined repressive effects of H3K27me3 and repressor 'R' action.

Among several models that might be postulated, we consider two to explain the derepression of some X-linked genes in *mes-4* mutants. (1) MES-4 normally activates the expression of an autosomally encoded repressor that selectively represses genes on the X chromosome (Fig. 8, upper right). The expression of four autosomal genes is, in fact, downregulated >1.8-fold in *mes-4* mutants. However, these genes do not possess motifs or show homologies that make them good candidates for serving as transcriptional repressors. Furthermore, RNAi depletion of each gene did not result in sterility (Gonczy et al., 2000; Kamath et al., 2003; Rual et al., 2004; Sonnichsen et al., 2005) (C.R.C. and S.S., unpublished). (2) An autosomal concentration of MES-4 or its H3K36me2 mark repels a global repressor, thereby concentrating repressor action on the X chromosomes (Fig. 8, lower right). We hypothesize that MES-2/MES-3/MES-6-catalyzed H3K27me3 concentrated on the X chromosome acts to repel MES-4 (Fig. 8, left), as suggested by the observation that MES-4 spreads onto the X chromosome in *mes-2*, *mes-3* and *mes-6* mutants (Fong et al., 2002) (this study), and that MES-4 and/or H3K36me2 concentrated on the autosomes repel an unidentified repressor ('R' in the figure). The possibility that this unidentified repressor is the MES-2/MES-3/MES-6 complex itself is unlikely, as the pattern of H3K27me3 catalyzed by that complex is not visibly altered in *mes-4* mutants (see Fig. S2E,F in the supplementary material).

We postulate two types of X repression: a direct mechanism mediated by MES-2/MES-3/MES-6, and a novel, indirect mechanism mediated by MES-4. Loss of MES-2/MES-3/MES-6 would lead to the loss of repressive histone modifications and to at least some desilencing of the X chromosome. Loss of MES-4 would lead to insufficient levels of global repressor (model 1, Fig. 8) or promiscuous binding of the global repressor to autosomal regions, and, if the repressor is in limiting supply, to titration of repressor away from the X chromosome, causing at least some desilencing of the X (model 2, Fig. 8). One might expect promiscuous binding of the repressor to also cause widespread repression of autosomal loci, which we did not observe. If there is a limited supply of repressor and it is distributed over potentially six times more chromatin (10 autosomes in addition to the 2 Xs) in *mes-4* mutants than in wild type, then the critical concentration of repressor needed for repression may not be achieved at most autosomal loci.

Our notion that MES-4 may have a role in repelling a global repressor from the five autosomes, thereby focusing repressor action on the X chromosome, has a precedent in van Leeuwen and Gottschling's proposed 'gaining specificity by preventing promiscuity' model for the function of the *S. cerevisiae* H3K79 HMT Dot1 (van Leeuwen and Gottschling, 2002). Dot1 methylates ~90% of H3K79 residues in the genome; notably, silent chromatin, which comprises ~10% of the genome, is hypomethylated at that residue. Loss of Dot1 function and H3K79 methylation causes the SIR silencing proteins to spread from normally silent chromatin into

euchromatin, and causes loss of silencing. This illustrates how a globally distributed histone modification can reduce nonspecific binding of silencers, and focus their binding and silencing effects to discrete domains.

MES-4 in the soma

Although MES-4 is not essential for the health and viability of somatic tissue (Capowski et al., 1991), recent studies of synMuv (for synthetic multivulva) genes have revealed a role for MES-4 in somatic cells (Unhavaithaya et al., 2002; Wang et al., 2005; Cui et al., 2006). Several synMuv class B mutants show a remarkable phenotype: somatic cells display germline traits, including expression of the germline marker PGL-1 and enhanced RNAi. Concomitant loss of *mes-4* function suppresses the 'ectopic germline traits' and other synMuv phenotypes, and in the case of *mep-1* suppresses its larval lethality. This has led to a model in which MES-4 participates in conferring germline identity on cells, and the synMuv B regulators suppress or antagonize that function in somatic cells, thus protecting their somatic fates (Unhavaithaya et al., 2002; Strome, 2005). MES-4 is not alone in serving that proposed role; other *mes* genes and genes encoding additional chromatin regulators show similar genetic interactions with synMuv B mutants (Unhavaithaya et al., 2002; Wang et al., 2005; Cui et al., 2006). The targets of MES-4 regulation in somatic cells, and the mechanism by which MES-4 and synMuv B chromatin regulators antagonize each other, remain to be determined.

We thank Steve Dunkelbarger and Sean Boyle for technical assistance, and Jason Lieb, Lily Shiue and members of the Strome lab for helpful discussions. The Caenorhabditis Genetics Center supplied some strains. This work was supported by NIH grants GM34059 (S.S.), GM65682 (V.R.), and GM068804 (Y.Z.), Purdue Cancer Center NCI Training Grant CA09634 (I.M.F.), the Walther Cancer Institute (S.D.B.), and a Sidney Kimmel Scholar Award (S.D.B.).

Supplementary material

Supplementary material for this article is available at http://dev.biologists.org/cgi/content/full/133/19/3907/DC1

References

Adhvaryu, K. K., Morris, S. A., Strahl, B. D. and Selker, E. U. (2005). Methylation of histone H3 lysine 36 is required for normal development in *Neurospora crassa*. *Eukaryot. Cell* **4**, 1455-1464.

Bannister, A. J., Schneider, R., Myers, F. A., Thorne, A. W., Crane-Robinson, C. and Kouzarides, T. (2005). Spatial distribution of di- and tri-methyl lysine 36 of histone H3 at active genes. *J. Biol. Chem.* **280**, 17732-17736.

Baugh, L. R., Hill, A. A., Slonim, D. K., Brown, E. L. and Hunter, C. P. (2003). Composition and dynamics of the *Caenorhabditis elegans* early embryonic transcriptome. *Development* **130**, 889-900.

Bean, C. J., Schaner, C. E. and Kelly, W. G. (2004). Meiotic pairing and imprinted X chromatin assembly in *Caenorhabditis elegans*. *Nat. Genet.* **36**, 100-105.

Bender, L. B., Cao, R., Zhang, Y. and Strome, S. (2004). The MES-2/MES-3/MES-6 complex and regulation of histone H3 methylation in *C. elegans*. *Curr. Biol.* **14**, 1639-1643.

Bienz, M. (2006). The PHD finger, a nuclear protein-interaction domain. *Trends Biochem. Sci.* **31**, 35-40.

Cao, R., Wang, L., Wang, H., Xia, L., Erdjument-Bromage, H., Tempst, P., Jones, R. S. and Zhang, Y. (2002). Role of histone H3 lysine 27 methylation in Polycomb-group silencing. *Science* **298**, 1039-1043.

Capowski, E. E., Martin, P., Garvin, C. and Strome, S. (1991). Identification of grandchildless loci whose products are required for normal germ-line development in the nematode *Caenorhabditis elegans*. *Genetics* **129**, 1061-1072.

Carrozza, M. J., Li, B., Florens, L., Suganuma, T., Swanson, S. K., Lee, K. K., Shia, W. J., Anderson, S., Yates, J., Washburn, M. P. et al. (2005). Histone H3 methylation by Set2 directs deacetylation of coding regions by Rpd3S to suppress spurious intragenic transcription. *Cell* **123**, 581-592.

Chi, W. and Reinke, V. (2006). Promotion of oogenesis and embryogenesis in the *C. elegans* gonad by EFL-1/DPL-1 (E2F) does not require LIN-35 (pRB). *Development* **133**, 3147-3157.

Cui, M., Kim, E. B. and Han, M. (2006). Diverse chromatin remodeling genes antagonize the Rb-involved synMuv pathways in *C. elegans*. *PLoS Genet.* **2**, e74 DOI: 10.1371/journal.pgen.0020074.

Czermin, B., Melfi, R., McCabe, D., Seitz, V., Imhof, A. and Pirrotta, V. (2002). *Drosophila* enhancer of Zeste/ESC complexes have a histone H3 methyltransferase activity that marks chromosomal Polycomb sites. *Cell* **111**, 185-196.

Eberharter, A., Vetter, I., Ferreira, R. and Becker, P. B. (2004). ACF1 improves the effectiveness of nucleosome mobilization by ISWI through PHD-histone contacts. *EMBO J.* **23**, 4029-4039.

Edgar, L. G., Wolf, N. and Wood, W. B. (1994). Early transcription in *Caenorhabditis elegans* embryos. *Development* **120**, 443-451.

Fang, J., Feng, Q., Ketel, C. S., Wang, H., Cao, R., Xia, L., Erdjument-Bromage, H., Tempst, P., Simon, J. A. and Zhang, Y. (2002). Purification and functional characterization of SET8, a nucleosomal histone H4-lysine 20-specific methyltransferase. *Curr. Biol.* **12**, 1086-1099.

Fire, A., Alcazar, R. and Tan, F. (2006). Unusual DNA structures associated with germline genetic activity in *Caenorhabditis elegans*. *Genetics* **173**, 1259-1273.

Fischle, W., Wang, Y. and Allis, C. D. (2003). Histone and chromatin cross-talk. *Curr. Opin. Cell Biol.* **15**, 172-183.

Fong, Y., Bender, L., Wang, W. and Strome, S. (2002). Regulation of the different chromatin states of autosomes and X chromosomes in the germ line of *C. elegans*. *Science* **296**, 2235-2238.

Garvin, C., Holdeman, R. and Strome, S. (1998). The phenotype of *mes-2*, *mes-3*, *mes-4* and *mes-6*, maternal-effect genes required for survival of the germline in *Caenorhabditis elegans*, is sensitive to chromosome dosage. *Genetics* **148**, 167-185.

Gonczy, P., Echeverri, C., Oegema, K., Coulson, A., Jones, S. J., Copley, R. R., Duperon, J., Oegema, J., Brehm, M., Cassin, E. et al. (2000). Functional genomic analysis of cell division in *C. elegans* using RNAi of genes on chromosome III. *Nature* **408**, 331-336.

Han, Z., Saam, J. R., Adams, H. P., Mango, S. E. and Schumacher, J. M. (2003). The *C. elegans* Tousled-like kinase (TLK-1) has an essential role in transcription. *Curr. Biol.* **13**, 1921-1929.

Hird, S. N., Paulsen, J. E. and Strome, S. (1996). Segregation of germ granules in living *Caenorhabditis elegans* embryos: cell-type-specific mechanisms for cytoplasmic localisation. *Development* **122**, 1303-1312.

Jiang, M., Ryu, J., Kiraly, M., Duke, K., Reinke, V. and Kim, S. K. (2001). Genome-wide analysis of developmental and sex-regulated gene expression profiles in *Caenorhabditis elegans*. *Proc. Natl. Acad. Sci. USA* **98**, 218-223.

Joshi, A. A. and Struhl, K. (2005). Eaf3 chromodomain interaction with methylated H3-K36 links histone deacetylation to Pol II elongation. *Mol. Cell* **20**, 971-978.

Kamath, R. S., Fraser, A. G., Dong, Y., Poulin, G., Durbin, R., Gotta, M., Kanapin, A., Le Bot, N., Moreno, S., Sohrmann, M. et al. (2003). Systematic functional analysis of the *Caenorhabditis elegans* genome using RNAi. *Nature* **421**, 231-237.

Kawasaki, I., Amiri, A., Fan, Y., Meyer, N., Dunkelbarger, S., Motohashi, T., Karashima, T., Bossinger, O. and Strome, S. (2004). The PGL family proteins associate with germ granules and function redundantly in *Caenorhabditis elegans* germline development. *Genetics* **167**, 645-661.

Kelly, W. G. and Fire, A. (1998). Chromatin silencing and the maintenance of a functional germline in *Caenorhabditis elegans*. *Development* **125**, 2451-2456.

Kelly, W. G., Schaner, C. E., Dernburg, A. F., Lee, M. H., Kim, S. K., Villeneuve, A. M. and Reinke, V. (2002). X-chromosome silencing in the germline of *C. elegans*. *Development* **129**, 479-492.

Keogh, M. C., Kurdistani, S. K., Morris, S. A., Ahn, S. H., Podolny, V., Collins, S. R., Schuldiner, M., Chin, K., Punna, T., Thompson, N. J. et al. (2005). Cotranscriptional Set2 methylation of histone H3 lysine 36 recruits a repressive Rpd3 complex. *Cell* **123**, 593-605.

Ketel, C. S., Andersen, E. F., Vargas, M. L., Suh, J., Strome, S. and Simon, J. A. (2005). Subunit contributions to histone methyltransferase activities of fly and worm polycomb group complexes. *Mol. Cell. Biol.* **25**, 6857-6868.

Kizer, K. O., Phatnani, H. P., Shibata, Y., Hall, H., Greenleaf, A. L. and Strahl, B. D. (2005). A novel domain in Set2 mediates RNA polymerase II interaction and couples histone H3 K36 methylation with transcript elongation. *Mol. Cell. Biol.* **25**, 3305-3316.

Krogan, N. J., Kim, M., Tong, A., Golshani, A., Cagney, G., Canadien, V., Richards, D. P., Beattie, B. K., Emili, A., Boone, C. et al. (2003). Methylation of histone H3 by Set2 in *Saccharomyces cerevisiae* is linked to transcriptional elongation by RNA polymerase II. *Mol. Cell. Biol.* **23**, 4207-4218.

Kuzmichev, A., Nishioka, K., Erdjument-Bromage, H., Tempst, P. and Reinberg, D. (2002). Histone methyltransferase activity associated with a human multiprotein complex containing the Enhancer of Zeste protein. *Genes Dev.* **16**, 2893-2905.

Li, B., Howe, L., Anderson, S., Yates, J. R., 3rd and Workman, J. L. (2003). The Set2 histone methyltransferase functions through the phosphorylated carboxyl-terminal domain of RNA polymerase II. *J. Biol. Chem.* **278**, 8897-8903.

Li, H., Ilin, S., Wang, W., Duncan, E. M., Wysocka, J., Allis, C. D. and Patel, D. J. (2006). Molecular basis for site-specific read-out of histone H3K4me3 by the BPTF PHD finger of NURF. *Nature* **442**, 91-95.

Li, J., Moazed, D. and Gygi, S. P. (2002). Association of the histone methyltransferase Set2 with RNA polymerase II plays a role in transcription elongation. *J. Biol. Chem.* **277**, 49383-49388.
MacQueen, A. J., Phillips, C. M., Bhalla, N., Weiser, P., Villeneuve, A. M. and Dernburg, A. F. (2005). Chromosome sites play dual roles to establish homologous synapsis during meiosis in *C. elegans*. *Cell* **123**, 1037-1050.
Martin, C. and Zhang, Y. (2005). The diverse functions of histone lysine methylation. *Nat. Rev. Mol. Cell Biol.* **6**, 838-849.
Monestier, M., Novick, K. E. and Losman, M. J. (1994). D-penicillamine- and quinidine-induced antinuclear antibodies in A.SW (H-2s) mice: similarities with autoantibodies in spontaneous and heavy metal-induced autoimmunity. *Eur. J. Immunol.* **24**, 723-730.
Morris, S. A., Shibata, Y., Noma, K., Tsukamoto, Y., Warren, E., Temple, B., Grewal, S. I. and Strahl, B. D. (2005). Histone H3 K36 methylation is associated with transcription elongation in *Schizosaccharomyces pombe*. *Eukaryot. Cell* **4**, 1446-1454.
Muller, J., Hart, C. M., Francis, N. J., Vargas, M. L., Sengupta, A., Wild, B., Miller, E. L., O'Connor, M. B., Kingston, R. E. and Simon, J. A. (2002). Histone methyltransferase activity of a *Drosophila* Polycomb group repressor complex. *Cell* **111**, 197-208.
Pena, P. V., Davrazou, F., Shi, X., Walter, K. L., Verkhusha, V. V., Gozani, O., Zhao, R. and Kutateladze, T. G. (2006). Molecular mechanism of histone H3K4me3 recognition by plant homeodomain of ING2. *Nature* **442**, 31-32.
Pfaffl, M. W. (2001). A new mathematical model for relative quantification in real-time RT-PCR. *Nucleic Acids Res.* **29**, e45.
Phillips, C. M., Wong, C., Bhalla, N., Carlton, P. M., Weiser, P., Meneely, P. M. and Dernburg, A. F. (2005). HIM-8 binds to the X chromosome pairing center and mediates chromosome-specific meiotic synapsis. *Cell* **123**, 1051-1063.
Ragvin, A., Valvatne, H., Erdal, S., Årskog, V., Tufteland, K. R., Breen, K., Øyan, A. M., Eberharter, A., Gibson, T. J., Becker, P. B. et al. (2004). Nucleosome binding by the bromodomain and PHD finger of the transcriptional cofactor p300. *J. Mol. Biol.* **337**, 773-788.
Rao, B., Shibata, Y., Strahl, B. D. and Lieb, J. D. (2005). Dimethylation of histone H3 at lysine 36 demarcates regulatory and nonregulatory chromatin genome-wide. *Mol. Cell. Biol.* **25**, 9447-9459.
Rayasam, G. V., Wendling, O., Angrand, P. O., Mark, M., Niederreither, K., Song, L., Lerouge, T., Hager, G. L., Chambon, P. and Losson, R. (2003). NSD1 is essential for early post-implantation development and has a catalytically active SET domain. *EMBO J.* **22**, 3153-3163.
Reinke, V., Smith, H. E., Nance, J., Wang, J., Van Doren, C., Begley, R., Jones, S. J., Davis, E. B., Scherer, S., Ward, S. et al. (2000). A global profile of germline gene expression in *C. elegans*. *Mol. Cell* **6**, 605-616.
Reinke, V., Gil, I. S., Ward, S. and Kazmer, K. (2004). Genome-wide germline-enriched and sex-biased expression profiles in *Caenorhabditis elegans*. *Development* **131**, 311-323.
Rual, J. F., Ceron, J., Koreth, J., Hao, T., Nicot, A. S., Hirozane-Kishikawa, T., Vandenhaute, J., Orkin, S. H., Hill, D. E., van den Heuvel, S. et al. (2004). Toward improving *Caenorhabditis elegans* phenome mapping with an ORFeome-based RNAi library. *Genome Res.* **14**, 2162-2168.
Schaft, D., Roguev, A., Kotovic, K. M., Shevchenko, A., Sarov, M., Neugebauer, K. M. and Stewart, A. F. (2003). The histone 3 lysine 36 methyltransferase, SET2, is involved in transcriptional elongation. *Nucleic Acids Res.* **31**, 2475-2482.
Schneider, R., Bannister, A. J. and Kouzarides, T. (2002). Unsafe SETs: histone lysine methyltransferases and cancer. *Trends Biochem. Sci.* **27**, 396-402.
Seydoux, G. and Fire, A. (1994). Soma-germline asymmetry in the distributions of embryonic RNAs in *Caenorhabditis elegans*. *Development* **120**, 2823-2834.
Shim, E. Y., Walker, A. K., Shi, Y. and Blackwell, T. K. (2002). CDK-9/cyclin T (P-TEFb) is required in two postinitiation pathways for transcription in the *C. elegans* embryo. *Genes Dev.* **16**, 2135-2146.
Sims, R. J., 3rd, Nishioka, K. and Reinberg, D. (2003). Histone lysine methylation: a signature for chromatin function. *Trends Genet.* **19**, 629-639.
Sonnichsen, B., Koski, L. B., Walsh, A., Marschall, P., Neumann, B., Brehm, M., Alleaume, A. M., Artelt, J., Bettencourt, P., Cassin, E. et al. (2005). Full-genome RNAi profiling of early embryogenesis in *Caenorhabditis elegans*. *Nature* **434**, 462-469.
Stillman, B. and Stewart, D. (ed.) (2004). *Epigenetics: Cold Spring Harbor Symposia on Quantitative Biology.* Vol. 69. Cold Spring Harbor, NY: Cold Spring Harbor Laboratory Press.
Strahl, B. D., Grant, P. A., Briggs, S. D., Sun, Z. W., Bone, J. R., Caldwell, J. A., Mollah, S., Cook, R. G., Shabanowitz, J., Hunt, D. F. et al. (2002). Set2 is a nucleosomal histone H3-selective methyltransferase that mediates transcriptional repression. *Mol. Cell. Biol.* **22**, 1298-1306.
Strome, S. (2005). Specification of the germ line. In *WormBook* (ed. The *C. elegans* Research Community), http://www.wormbook.org.
Strome, S. and Wood, W. B. (1983). Generation of asymmetry and segregation of germ-line granules in early *C. elegans* embryos. *Cell* **35**, 15-25.
Sun, X. J., Wei, J., Wu, X. Y., Hu, M., Wang, L., Wang, H. H., Zhang, Q. H., Chen, S. J., Huang, Q. H. and Chen, Z. (2005). Identification and characterization of a novel human histone H3 lysine 36-specific methyltransferase. *J. Biol. Chem.* **280**, 35261-35271.
Tsukada, Y., Fang, J., Erdjument-Bromage, H., Warren, M. E., Borchers, C. H., Tempst, P. and Zhang, Y. (2006). Histone demethylation by a family of JmjC domain-containing proteins. *Nature* **439**, 811-816.
Unhavaithaya, Y., Shin, T. H., Miliaras, N., Lee, J., Oyama, T. and Mello, C. C. (2002). MEP-1 and a homolog of the NURD complex component Mi-2 act together to maintain germline-soma distinctions *in C. elegans*. *Cell* **111**, 991-1002.
van Leeuwen, F. and Gottschling, D. E. (2002). Genome-wide histone modifications: gaining specificity by preventing promiscuity. *Curr. Opin. Cell Biol.* **14**, 756-762.
Wang, D., Kennedy, S., Conte, D., Jr, Kim, J. K., Gabel, H. W., Kamath, R. S., Mello, C. C. and Ruvkun, G. (2005). Somatic misexpression of germline P granules and enhanced RNA interference in retinoblastoma pathway mutants. *Nature* **436**, 593-597.
Whetstine, J. R., Ceron, J., Ladd, B., Dufourcq, P., Reinke, V. and Shi, Y. (2005). Regulation of tissue-specific and extracelluluar matrix-related genes by class I histone deacetylase. *Mol. Cell* **18**, 483-490.
Xiao, T., Hall, H., Kizer, K. O., Shibata, Y., Hall, M. C., Borchers, C. H. and Strahl, B. D. (2003). Phosphorylation of RNA polymerase II CTD regulates H3 methylation in yeast. *Genes Dev.* **17**, 654-663.
Xu, L. and Strome, S. (2001). Depletion of a novel SET-domain protein enhances the sterility of *mes-3* and *mes-4* mutants of *Caenorhabditis elegans*. *Genetics* **159**, 1019-1029.
Xu, L., Fong, Y. and Strome, S. (2001). The *Caenorhabditis elegans* maternal-effect sterile proteins, MES-2, MES-3, and MES-6, are associated in a complex in embryos. *Proc. Natl. Acad. Sci. USA* **98**, 5061-5066.

Table S1. Lesions in the seven alleles of *mes-4*

Allele	Nucleotide change*	Predicted protein change	Domain affected	H3K36me2 signal†
bn50	$TG_{540}T \rightarrow TAT$	C147Y	PHD I	Undetectable
bn67	$C_{765}AT \rightarrow TAT$	H206Y	PHD I	Undetectable
bn58	$C_{1362}GT \rightarrow TGT$	R389C	between PHD III and SET	Weak
bn85‡	Δnt2418-3540, from within intron 6 to within intron 8	Δaa591-768 (Δexons 7 and 8)	SET and post-SET	Undetectable
bn73	$TAT_{2687} \rightarrow TAA$	Y594Z	Protein undetectable	Undetectable
bn23§	$AG_{3130} \rightarrow AA$ at 3′ end of intron 7	Unknown	Protein undetectable	Undetectable
bn87¶	Δnt4006-5201, from within exon 10 past the 3′-UTR	Δaa877 onward	Protein undetectable	Undetectable

Lesions in *bn23*, *bn73*, and *bn87* were reported previously (Fong et al., 2002).

*Nucleotide position 1 is the A of the start codon.

†Anti-H3K36me2 antibody signal in early embryos and distal germ lines of adults. As expected, both the chromosomal association of MES-4 and the integrity of the SET domain apparently are required for its HMT activity.

‡*bn85* has an ~1.1 kb deletion that removes the region from the middle of intron 6 to the middle of intron 8. If splicing occurs between the 5′ end of intron 6 and the 3′ end of intron 8, then only exons 7 and 8 are missing. This in-frame deletion is predicted to produce a protein of 720 amino acids. A truncated MES-4 protein of approximately the expected size (178 amino acids or ~20 kDa smaller than wild type) is seen by western blot analysis of *mes-4(bn85)* worms (S. Boyle and L.B.B., unpublished), and protein accumulation in nuclei is seen by immunofluorescence.

§*bn23* has a point mutation that affects the conserved nucleotides at the 3′ end of intron 7. If splicing can occur between the 5′ end of intron 7 and the 3′ end of intron 8, then an in-frame protein missing only exon 8 (44 amino acids) is predicted. No protein is observed by immunofluorescence, suggesting that an altered splicing pattern produces an unstable mRNA and/or protein.

¶*bn87* has an ~1.2 kb deletion that removes the 3′ end of exon 10 and all of the 3′-UTR. The absence of protein product by immunofluorescence suggests that gene products are not synthesized or are not stable.

Table S2. Microarray results for the 71 genes whose accumulation is affected at least 1.8-fold (P<0.05)

Genes upregulated in *mes-4* relative to wild type

Primer pair	WormBase ID (gene name)	Chromosome	Genomic start position	*mes-4*/wt	*P*-value
F11A6.2	F11A6.2	I	11,682,352	1.9	0.02
M142.1	M142.1 (unc-119)	III	10,906,347	1.97	0.01
C17B7.11	C17B7.11 (fbxa-65)	V	3,346,310	1.87	0.0093
W09B7.B	W09B7.2	V	8,827,969	2.03	0.015
C18D4.6	C18D4.6	V	17,538,168	2.59	0.021
F25E5.1	F25E5.1	V	7,465,706	1.89	0.0037
C04E7.2	C04E7.2	X	353,620	1.88	0.0025
T04G9.3	T04G9.3 (ile-2)	X	768,594	2.05	0.017
F53H8.1	F53H8.1 (apm-3)	X	954,994	2.16	0.03
T26C11.6	T26C11.6 (ceh-21)	X	1,852,730	1.99	0.000044
F07D10.1	F07D10.1 (rpl-11.2)	X	2,242,613	2.1	0.024
F32E4.8	F52E4.8	X	3,102,150	1.85	0.0036
C15C7.1	C15C7.1	X	3,164,514	1.82	0.0012
F35A5.8	F35A5.8 (erp-1)	X	3,802,751	2.84	0.00031
F02E8.1	F02E8.1 (asb-2)	X	4,469,739	1.81	0.0072
C05E11.1	C05E11.1	X	4,588,738	1.92	0.0027
T13H2.4	T13H2.4 (pqn-65)	X	4,620,394	1.82	0.0012
Y34B4A.F	Y34B4A.2	X	5,279,588	1.94	0.0041
F32A6.3	F32A6.3 (vps-41)	X	5,283,796	2.66	0.0017
C54H2.5	C54H2.5 (sft-4)	X	5,780,680	2.08	0.0029
F46G11.3	F46G11.3	X	5,783,363	2.21	0.00064
R07E4.5	R07E4.5	X	5,953,132	1.86	0.026
C09B8.7	C09B8.7 (pak-1)	X	6,048,568	3.3	0.00016
C45B2.6	C45B2.6	X	6,053,058	2.42	0.00052
T13C5.5	T13C5.5 (bca-1)	X	6,206,433	2.67	0.0003
T13C5.6	T13C5.6	X	6,207,584	2.47	0.00085
C03B1.12	C03B1.12 (lmp-1)	X	6,377,643	1.84	0.0028
C36B7.6	C36B7.6	X	7,100,289	1.97	0.000073
F08C6.6	F08C6.6	X	7,569,666	1.83	0.0092
ZK154.7	ZK154.7 (adm-4)	X	7,798,227	2.03	0.0098
F13B9.8	F13B9.8 (fis-2)	X	8,285,157	1.97	0.0051
R09F10.3	R09F10.3	X	8,294,561	1.97	0.0003
F08F1.7	F08F1.7	X	8,421,993	2.47	0.011
C25A11.1	C25A11.1	X	9,119,846	3.46	0.00014
B0416.5	B0416.5	X	9,270,784	2.31	0.0029
B0416.6	B0416.6 (gly-13)	X	9,296,553	2.25	0.001
T20B5.1	T20B5.1 (apa-2)	X	9,336,750	2.3	0.00042
T09B9.4	T09B9.4	X	9,774,286	2.21	0.0038
F47B10.1	F47B10.1	X	10,900,040	2.72	0.0017
W04G3.5	W04G3.5	X	11,073,581	1.85	0.001
C34F6.4	C34F6.4 (hst-2)	X	11,207,015	1.96	0.016
C35C5.6	C35C5.6	X	11,563,910	1.86	0.00042
F54F7.6	F54F7.6	X	11,865,464	2.33	0.000037
VW06B3R.1	VW06B3R.1	X	12,018,349	1.96	0.012
VF11C1L.1	VF11C1L.1 (ppk-3)	X	12,974,958	1.95	0.005
F54B11.5	F54B11.5	X	13,595,987	2.08	0.0038
Y26E6A.1	Y26E6A.1	X	13,917,091	1.8	0.0018
C31E10.5	C31E10.5	X	13,995,987	1.84	0.0045
F28H6.4	F28H6.4	X	14,127,802	2.01	0.00092
C27C12.1	C27C12.1	X	14,853,672	2.44	0.016
C27C12.4	C27C12.4	X	14,854,072	1.8	0.027
C27C12.3	C27C12.3	X	14,865,762	2.35	0.0092
F31F6.1	F31F6.1	X	14,868,218	2.13	0.03
F20D1.1	F20D1.1	X	14,970,190	2.24	0.016
F20D1.2	F20D1.2	X	14,970,668	2.43	0.00084
F20D1.3	F20D1.3	X	14,976,032	2.52	0.00053
F20D1.6	F20D1.6 (rbg-1)	X	14,983,442	1.84	0.0074
H40L08.1	H40L08.1	X	15,083,879	2.29	0.003
R03A10.4	R03A10.4	X	15,441,648	1.83	0.039
K09A9.5	K09A9.5 (gas-1)	X	15,590,318	2.3	0.011
K09A9.1	K09A9.1	X	15,607,888	2.08	0.0079
ZK678.1	ZK678.1 (lin-15A)	X	15,731,887	2.06	0.034
F59F4.4	F59F4.4 (acl-1)	X	15,849,818	1.93	0.016
F31B9.3	F31B9.3	X	15,923,396	2.05	0.00043
F01G12.2	F01G12.2 (sur-7)	X	16,376,514	2.06	0.007
C33E10.2	C33E10.2 (fbxa-120)	X	17,302,664	2.83	0.00024
H11L12.1	H11L12.1	X	17,711,584	2.21	0.0025

Genes downregulated in *mes-4* relative to wild type

Primer pair	WormBase ID (gene name)	Chromosome	Genomic start position	wt/*mes-4*	*P*-value
C16A3.10	C16A3.10	III	6,396,119	2.23	0.0036
F57G4.4	F57G4.4	V	17,639,720	1.84	0.0061
F57G4.8	F57G4.8	V	17,650,317	2.2	0.0026
F59A1.9	F59A1.9	V	17,655,076	1.95	0.0078

Table S3. Comparison of microarray results and real-time PCR results for 15 genes

Genes upregulated at least 1.8-fold (*P*<0.05) in *mes-4* relative to wild type

					Real-time PCR relative to:	
Primer pair	WormBase ID (gene name)	Chromosome	*mes-4*/wt	*P*-value	ZK381.1	F14B4.2
F11A6.2	F11A6.2	I	1.9	0.02	12.95	11.72
C17B7.11	C17B7.11 (fbxa-65)	V	1.87	0.0093	2.88	2.89
F25E5.1	F25E5.1	V	1.89	0.0037	6.13	6.83
C09B8.7	C09B8.7 (pak-1)	X	3.3	0.00016	10.44	9.79
T13C5.6	T13C5.6	X	2.47	0.00085	7.34	8.19
F08F1.7	F08F1.7	X	2.47	0.011	8.06	8.07
C25A11.1	C25A11.1	X	3.46	0.00014	16.99	18.96
R03A10.4	R03A10.4	X	1.83	0.039	6.3	6.31
H11L12.1	H11L12.1	X	2.21	0.0025	14.69	13.77

Gene downregulated at least 1.8-fold (*P*<0.05) in *mes-4* relative to wild type

					Real-time PCR relative to:	
Primer pair	WormBase ID (gene name)	Chromosome	wt/*mes-4*	*P*-value	ZK381.1	14B4.2
F57G4.8	F57G4.8	V	2.2	0.0026	3.71	3.74

Genes with approximately equivalent accumulation in *mes-4* and wild type

					Real-time PCR relative to:	
Primer pair	WormBase ID (gene name)	Chromosome	wt/*mes-4*	*P*-value	ZK381.1	F14B4.2
F14B4.2	F14B4.2	I	1.15	0.0038	1.01	
F49D11.8	F49D11.8 (cpn-4)	I	1.04	0.0053	1.47	1.84
B0361.8	B0361.8	III	1.04	0.0069	0.92	1.14
ZK381.1	ZK381.1 (him-3)	IV	1.18	0.091		0.99
K07C11.2	K07C11.2 (air-1)	V	0.94	0.032	1.14	1.27

As described in the Materials and methods, RNA was isolated from 50 dissected gonads per genotype. It was not linearly amplified. Real-time PCR was performed in triplicate for each gene indicated, relative to two reference genes (ZK381.1 and F14B4.2).